DOI: 10.1002/ejic.200800975

Mechanism of Hydride Abstraction by Cyclopentadienone-Ligated Carbonylmetal Complexes (M = Ru, Fe)

Megan K. Thorson,[a] Kortney L. Klinkel,[a] Jianmei Wang,[a] and Travis J. Williams*[a]

Keywords: Cyclopentadienone ligands / C–H bond activation / Oxidation / Hydrides / Reaction mechanisms

Cyclopentadienone-ligated ruthenium complexes, such as Shvo's catalyst, are known to oxidize reversibly alcohols to the corresponding carbonyl compounds. The mechanism of this reaction has been the subject of some controversy, but it is generally believed to proceed through concerted transfer of proton and hydride, respectively, to the cyclopentadienone ligand and the ruthenium center. In this paper we further study the hydride transfer process as an example of a coordinatively directed hydride abstraction by adding quantitative understanding to some features of this mechanism that are not well understood. We find that an oxidant as weak as acetone can be used to re-oxidize the intermediate ruthenium hydride without catalyst re-oxidation becoming rate-limiting. Furthermore, C–H cleavage is a significantly electrophilic event, as demonstrated by a Hammett reaction parameter of $\rho = -0.89$. We then describe how the application of our mechanistic insights obtained from the study have enabled us to extend the ligand-directed hydride abstraction strategy to include a rare example of an iron(0) oxidation catalyst.

Introduction

C–H bond oxidation by hydride abstraction is an important reaction for organic synthesis and has a central role in applications ranging from utilization of hydrocarbon feedstocks to fine chemical synthesis,[1] yet its mechanism is underexplored and its applications are scarcely exploited. Our group is developing ligand–metal bifunctional catalysts for hydride abstraction from general organic substrates to enable nucleophilic substitution reactions in which hydride is activated as a leaving group (Scheme 1, A). Our strategy is to devise a bifunctional catalyst in which the ligand "addresses" the catalyst to a particular C–H bond by placing an electrophilic metal atom in its immediate proximity. Following hydride transfer to metal atom, the resulting M–H group must be re-oxidized under mild conditions.

We have adopted the cyclopentadienone-ligated metal scaffold (e.g. **3**) as a starting point for development of coordination-directed hydride abstraction reactions because of the apparently significant role of the cyclopentadienone as a redox non-innocent ligand. "Shvo's catalyst" (Scheme 1, **1**),[2] is an example of this type of reactivity. Compound **1** itself, an air-stable, commercially available, crystalline solid, is the heterodimer of reduced (**2**) and oxidized (**3**) forms. The mixture of **2** and **3**, generated by dissociation of **1**, is known to catalyze reversibly the interconversion of carbonyl and alcohol compounds (Scheme 1, C). Although **1** was first introduced as a hydrogenation catalyst, its utility in the corresponding oxidation reaction has also been examined.[1f,3] Data collected to date regarding the mechanism of oxidation reactions catalyzed by **1** are most consistent with a mechanism involving transfer of both hydrogen atoms (O–H and C–H) in or before a single rate-determining transition state when the reaction is conducted under strongly oxidative conditions (tetrafluorobenzoquinone).[3b] Thus, **3** is a bifunctional metal–ligand scaffold in which H^+ (from O–H) acts as a coordinating direction element "L" that disposes an electrophilic ruthenium center "M^+" in the proximity of a C–H bond.

We believe that coordination-directed hydride abstraction will be an excellent strategy for our program of designing and developing efficient, selective, inexpensive, and environmentally benign catalysts for C–H oxidation, and we believe that identification of mild conditions of re-oxidation of metal hydrides (such as **2**) will be essential to the identification of high-value catalytic systems because this is a key to realizing catalytic turnover. Moreover, an improved understanding of the polarization and energetics of hydride abstraction mediated at a cyclopentadienone-ligated metal center (such as **3**) is essential to effective catalyst design. In this paper we address these issues for the case of some Shvo-related complexes, and add quantitative understanding to some features of this mechanism that are a key to our goal (Scheme 1, A): *an oxidant as weak as acetone can be used, and catalyst re-oxidation does not become rate-limiting; replacement of a single phenyl group of*

[a] Loker Hydrocarbon Research Institute and Department of Chemistry, University of Southern California,
837 Bloom Walk, Los Angeles, CA 90089-1661, USA
Fax: +1-213-740-6679
E-mail: travisw@usc.edu

Supporting information for this article is available on the WWW under http://www.eurjic.org or from the author.

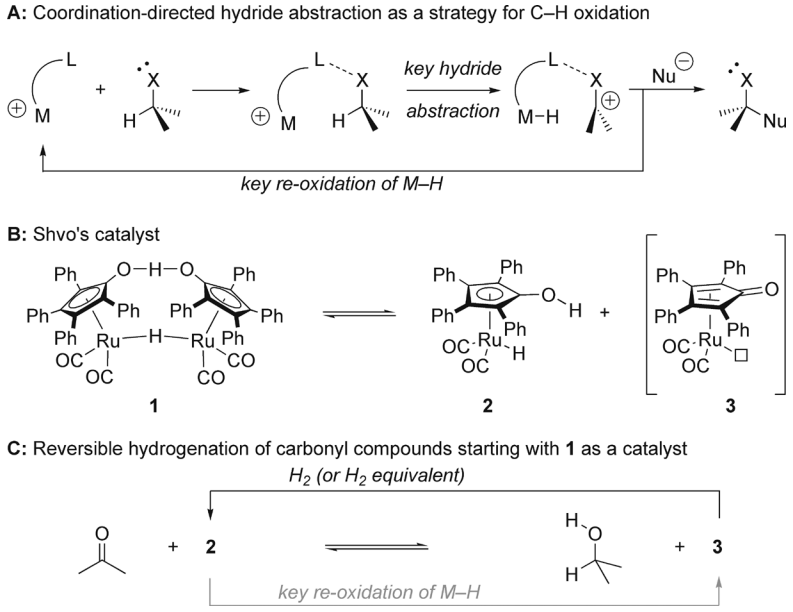

Scheme 1. Shvo's system as a platform for hydride abstraction reactions.

the cyclopentadienone ring can reduce the efficiency of oxidation significantly; and C–H cleavage is a significantly electrophilic event. We then describe how the application of this weakly oxidizing medium and our mechanistic insights obtained from the study have enabled us to extended the strategy to include a *rare example of an iron(0)-based oxidation catalyst*.

Results and Discussion

Studies on **1** conducted by Shvo et al.,[2] Casey et al.,[4] Bäckvall et al.,[1f,3] and others[5] have shown that in aromatic solvents the catalyst resting state in these reactions is dimer **1**, which must dissociate to reduced (**2**) and oxidized (**3**) forms (very small K_1) for a reaction to occur. Alcohol oxidation with **1** has isotope effects on both C–H (k_H/k_D = 2.6) and O–H (k_H/k_D = 1.8).[3b] Bäckvall et al. have explained that these kinetic isotope effect (KIE) data, along with a k_H/k_D value of 4.61 for a fully deuterated substrate is consistent with a concerted transition state for hydride and proton transfer (Scheme 2).[3b]

We started our study by switching to acetone, a milder, environmentally more benign medium to effect oxidation with catalyst **1**. Upon dissolving dimer **1** in [D_6]acetone with alcohol **6a**, we find dissociation and oxidation of dimer **1** as is evident from the disappearance of the characteristic μ^2-H peak (δ = –18.1 ppm) and appearance of [D_6]2-propanol (δ = +3.9 ppm), which indicates that the dissoci-

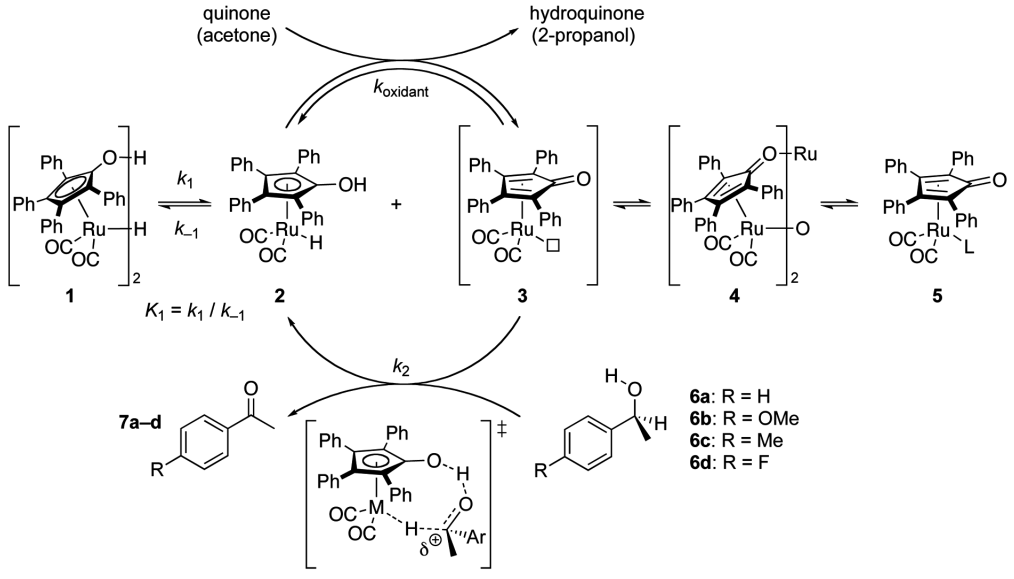

Scheme 2. Alcohol oxidation in Shvo's system.

ation equilibrium of **1** lies to the right under these conditions. This transformation is complete within the first acquisition of a kinetics run (see Supporting Information for an illustration). We perceive that the result is an acetone- or substrate-ligated dicarbonylruthenium complex (**5**, L = [D_6]acetone or **6**). Using this catalyst, we verify that **6a** can be converted to **7a** in 97% isolated yield on a 1 mmol scale.[6]

Systematic kinetics experiments on the conversion of **6a** to **7a** (Table 1) in [D_6]acetone solution support a rate law of $d[\mathbf{6a}]/dt = -k_2 \cdot [\mathbf{1}]^{1/2} \cdot [\mathbf{6a}]^1 \cdot [\text{oxidant}]^0$ with $k_2 = 1.67(6) \times 10^{-2}$ M$^{-1/2}$ s^{-1}. This is analogous to what Bäckvall et al. observed for quinone conditions (**1**, [D_6]benzene, tetrafluorobenzoquinone), but is interesting because we observe no kinetic order in the re-oxidation step even though it is a significantly milder oxidant than tetrafluorobenzoquinone. Kinetic order on [**1**] is illustrated in a plot of ln(k_{obs}) versus ln[**1**] (Figure 1, left). A slope of 0.40(6) in this plot is consistent with a half-order dependence on [**1**]. This indicates that dimerization of **2** and **3** is occurring during the catalysis even though this equilibrium lies well to the right under the reaction conditions. The dependence of the reaction rate on [acetone] is shown graphically in Figure 1 (right). The observed rate constants (k_{obs}) decrease only slightly with [acetone] in a mixed [D_2]dichloromethane/[D_6]acetone solution. The high y intercept of this plot is inconsistent with the kinetic order on [acetone], but is more likely interpreted as a medium effect: the data in Figure 1 (right) represent variation from 25% to 100% acetone. This means that re-oxidation of **2** from **3** does not impact the rate of the overall reaction, and thus that [D_6]acetone is as efficient as a quinone in regenerating **3** from **2** in a solution.

In cases in which we introduced benzoquinone to compete with acetone in acetone solution (Table 1, Entries 4 and 5), acetone was the major oxidant because of its high concentration. By comparison of ^{1}H NMR peaks for benzoquinone and [D_6]2-propanol, we can estimate the ratio of rates of reduction of benzoquinone and acetone ($k_{BQ}/k_{acetone}$) as 414(4). Although we observe this ratio to be constant over the course of the conversion, we must interpret it as an upper bound because [D_6]2-propanol can reduce benzoquinone (by re-formation of [D_6]acetone) in the presence of **1**. Moreover, Table 1 (Entry 5) shows that an excess of quinone can slow the reaction. We perceive that this is a result of competitive binding of **3** by benzoquinone or hydroquinone.

An internal competition isotope effect experiment with [D]benzyl alcohol [PhC(D)HOH] afforded a value of k_H/k_D = 3.7(2) at 323 K through the first 40% of conversion. We assign our value to a primary KIE [as opposed to an equilibrium isotope effect (EIE) or a combination of both] because it is constant over the course of conversion. This value is higher than a literature value[3b] (k_H/k_D = 2.6 by independent runs) observed for the conversion of **6d** to **7d**, possibly because of the relative strength of the primary (versus secondary) C–H bond. The difference in these values can also be attributed to the role of an EIE in the literature measurement. By contrast, we observe full dissociation of **1**.

We also show that the C–H cleavage is an electrophilic event by measuring a Hammett ρ value of –0.89(5) by comparing the rates of oxidation of alcohols **6a**–**6d** in independent runs (Figure 2).[7] A Hammett reaction parameter of ρ = –0.89 is larger than expected for a transition state involving β-hydride elimination or free-radical hydrogen atom transfer. Kaneda et al. report ρ = –0.43 for the oxidation of **6** with a ruthenium catalyst immobilized on hydroxyapatite and proposes a β-hydride elimination mechanism.[8] Kuriacose et al. report ρ = –0.3 for the same reaction with a

Table 1. Kinetics data for the **1**-catalyzed conversion of **6a** to **7a**.[a]

Entry	k_{obs} ($\times 10^5$ s^{-1})	[**1**] [mM]	[**6a**] [mM]	BQ [mM]	$k_{BQ}/k_{acetone}$
1	7.55(26)	1.5	120	0	–
2	11.1(1)	2.9	120	0	–
3	7.46(3)	1.5	240	0	–
4	8.49(31)	1.5	120	72	410
5	4.13(7)	1.5	120	144	418

[a] $k_{obs} = k_2 \cdot [\mathbf{6}]$. BQ = benzoquinone; $k_2 = 1.67(6) \times 10^{-2}$ M$^{-1/2}$ s^{-1}.

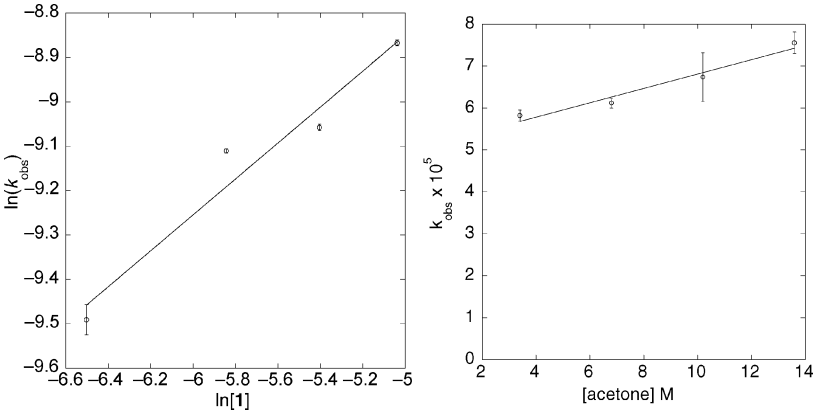

Figure 1. Left: plot of ln(k_{obs}) versus ln[**1**]; slope = 0.40(6). Right: plot of k_{obs} versus [acetone] in a mixed medium of [D_6]acetone and [D_2]dichloromethane. Kinetics data were processed as described in the Exp. Sect.

ruthenium trichloride catalyst in the presence of *N*-methylmorpholine *N*-oxide. These authors propose a hydrogen atom (radical) abstraction by an (oxoido)ruthenium(V) intermediate.[9] Our observation is more in line with benzyl alcohol oxidation by quinolinium chlorochromate (ρ = –1.2).[10] Thus, with catalyst **1**, we interpret that a significant cationic character is evolved at the carbon atom in the rate-determining transition state, which is only slightly compensated by electron donation from the concurrent deprotonation of the O–H bond.

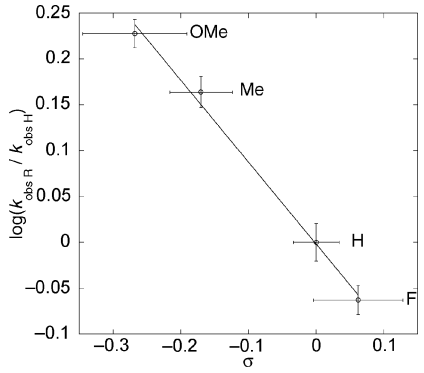

Figure 2. Hammett plot for the **1**-catalyzed conversion of **6** to **7**. Kinetics data were acquired and processed as described in the Exp. Sec. ρ = –0.89(5).

Furthermore, we have studied other ruthenium complexes based on electronically differentiated cyclopentadienones to compare the reaction rates. We attempted to prepare catalyst precursors analogous to **4** by treating $[Ru_3(CO)_{12}]$[4b] with the corresponding cyclopentadienone **9**[11] (Table 2). Only methyl-substituted compound **9b** participated in the formation of **4b** cleanly. Surprisingly, although **4b** appears monomeric under the reaction conditions used in Table 1, it reacts with **6a** ca. 10^1 times slower than the parent (**1**). Because **4b** is only sparingly soluble acetone, the experiment was repeated in a solvent system of $[D_2]$dichloromethane/$[D_6]$acetone (1:1). Under these conditions, both **1** and **4b** are completely dissolved and dissociated to active forms, and the parent system is only 60% faster: k_2(Ph)/k_2(Me) = 1.6(1). We observe, however, that the methyl-substituted system stalls at 46(1)% conversion, whereas the parent reached 92(3)%. This, along with a dark color that develops over time, indicates that the cyclopentadienone ligand is being lost in the course of the reaction. We thus assign the deficiencies of **4b** as: (1) solubility, (2) stability, and (3) rate in the C–H oxidation step (k_2). We further hypothesized that a more electron-deficient catalyst based on chloroalkyne **8c** would facilitate hydride abstraction and afford a faster oxidation reaction, but this complex is apparently unreactive (Scheme 3).

Table 2. Conversion of **6a** to **7a** with catalyst precursors **1** (gray) and **4b** (black).[a]

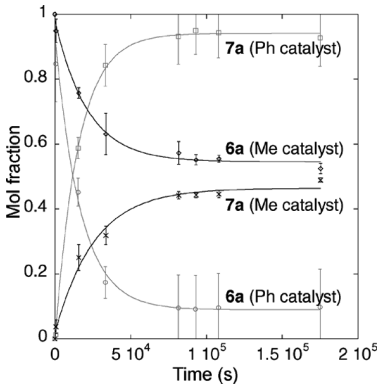

Entry	[Ru] source	k_{obs} ($\times 10^5$ s^{-1})	Conversion
1	**1** (gray)	6.3(2)	92(3)%
2	**4b** (black)	4.0(3)	46(1)%

[a] A solvent system of $[D_2]$dichloromethane/$[D_6]$acetone (1:1) was used.

Having identified mild oxidative conditions in which catalyst **1** operates smoothly, and having developed an understanding of the mechanistic details of the reaction under these conditions, we turned our attention to the possibility of replacing the catalytic ruthenium atom by an iron atom. To do so would involve hydride abstraction to a formal iron(0) center. Although biological oxidases such as cytochrome p450[12] rely on iron-based oxidation systems, these and related non-heme iron-based oxidation catalysts[13] generally feature an iron(II) or iron(III) precursor that is supported by several nitrogen ligands. These systems typically activate C–H bonds through the generation of a high-valent (oxido)iron intermediate[13c] from which hydrogen atoms (not hydride ions) are abstracted in a radical (or radical rebound) mechanism.[13a,13b] Several outstanding examples of C–H oxidation have been reported recently based on this strategy.[14] An iron homolog of **1**, however, would be structurally and mechanistically distinct: such a system would be supported by a redox-noninnocent cyclopentadienone li-

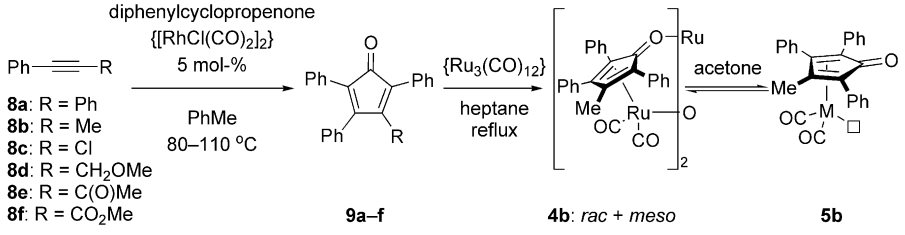

Scheme 3. Syntheses of **9** and **4**.

gand that would be an integral part of the catalyst's ligand–metal bifunctional nature, and C–H abstraction would involve transfer of a hydride ion, rather than a hydrogen radical. More closely related to our strategy are some examples of iron-catalyzed transfer hydrogenation catalysts in which a secondary alcohol is the hydrogen source. Some examples include a porphyrin-ligated system,[15] $[(PP3)Fe(H)(H_2)]^+$ $[BPh_4]^-$ [PP3 = $P(CH_2CH_2PPh_3)_3$],[16] and a cyclopentadienone-based system.[17] The first two appear to have little homology with our system, but the third suggests a starting point.

Surprisingly, (cyclopentadienone)iron(0) complexes do participate in productive hydride abstraction reactions in oxidative media. We first investigated this by preparing bicyclic complex **11** (Scheme 4)[18] and treating it with benzoquinone and alcohol **6a** in [D_6]benzene, which afforded only a trace amount of **7a** (Table 3, Entry 1). Curiously, we observe neither iron oxide formation nor ligand displacement from **11** under these conditions. Data in Table 2 suggested that this system could be improved by switching from doubly arylated complex **11** to fully phenylated complex **12**.[19] This worked moderately (Entry 2) and enabled a yield of 24%. Much as in the case of **1**, application of acetone conditions for re-oxidation of our catalyst is advantageous. In this case, a yield of 38% of **7a** is realized (Entry 3). As predicted by Hammett analysis, rate, and thus conversion, are higher with alcohol **6b**: this substrate can be oxidized in up to 79% yield of **7b**.

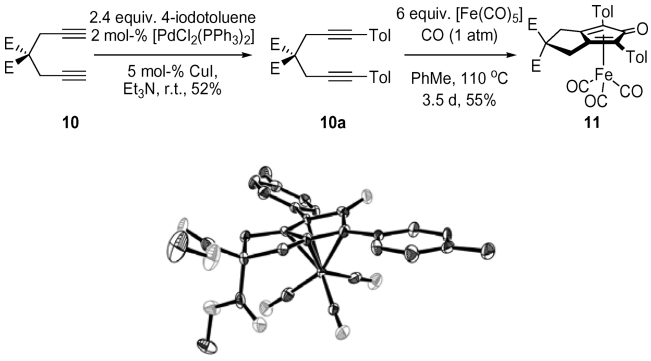

Scheme 4. Syntheses and X-ray structure of **11**.[20] E = CO_2Me.

Although significant improvement remains to be made in the efficiency of this iron(0)-based oxidation system, we have gathered some data regarding its mechanism. An iso-

Table 3. Iron-catalyzed conversion of **6** to **7**.[a]

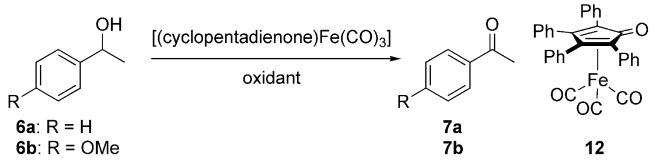

Entry	[Fe]	Alcohol	Oxidant	Solvent	*T* [°C]	Yield (conv.), time
1	11 (0.1 equiv.)	**6a**	BQ	C_6D_6	65	1% (1%), 16 h
2	12 (0.1 equiv.)	**6a**	BQ	C_6D_6	65	11% (14%), 17 h 24% (26%), 4 d
3	12 (0.1 equiv.)	**6a**	–	$(CD_3)_2CO$	54	38% (44%), 4 d
4[b]	12 (0.2 equiv.)	**6b**	–	$(CD_3)_2CO$	80	52% (79%), 4 d
5[b]	12 (0.5 equiv.)	**6b**	–	$(CD_3)_2CO$	80	79% (97%), 2 d

[a] Yield and conversion were determined by NMR spectroscopy. BQ = benzoquinone. All reactions were run in screw-capped NMR tubes and prepared in air. [b] Experiments 4 and 5 were run with 1 equiv. (relative to **12**) of D_2O at 80 °C (bath temp.) in a J. Young NMR tube under reduced pressure after rigorous degassing.

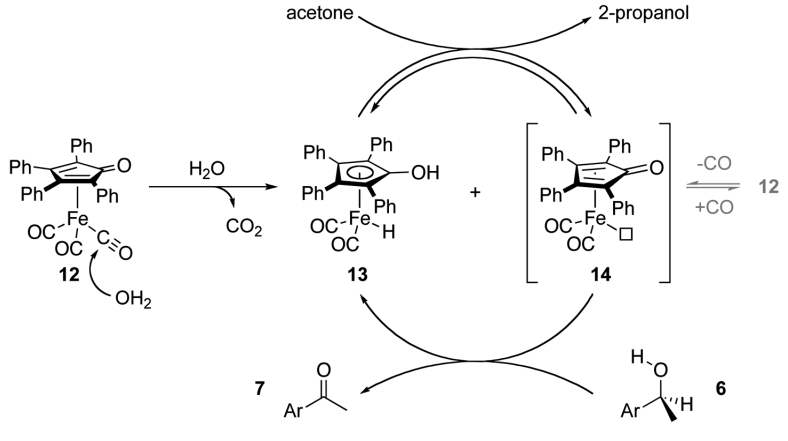

Scheme 5. Proposed mechanisms for alcohol oxidation with catalyst precursor **12**.

tope effect (determined as above through 20% conversion at 50 °C) of 3.6(9) indicates that C–H bond cleavage occurs in the rate-limiting step. The relative facility of oxidation of **6b** relative to **6a** is consistent with the view that this cleavage is an electrophilic event, as is observed in the ruthenium system. To the extent that direct comparison is possible, iron-based system **12** is slower than ruthenium-based system **1**. In both cases, we perceive that the active catalytic species is a dicarbonyl(cyclopentadienone)metal complex (**14** or **3**) and that hydride abstraction by that species is rate-determining. For alcohol **6a**, we observe an initial turnover frequency of 7.8(1) h^{-1} for ruthenium (**1**-based) and 0.10(1) h^{-1} for iron (**12**-based) under analogous conditions. Although we believe that this reflects the relative energetics of hydride abstraction, an induction period for the initiation of **12** cannot be excluded.

Because complexes **11** and **12** are coordinatively saturated species (18 electrons), these are most likely precursors that enter a catalytic cycle by ligand dissociation. We perceive based on previous literature[17b] that the mechanism of activation involves hydrolysis of one CO ligand to give CO_2 and intermediate **13** (Scheme 5). Thermal or photochemical dissociation of CO from **12** (highlighted in gray) is also a possibility. Once initiated, we believe that this mechanism proceeds analogously to Scheme 2.

Conclusions

Herein we describe mechanistic paradigms regarding the oxidation of alcohols with cyclopentadienone-ligated metal catalysts that are a key to our ongoing program in directed hydride abstraction: alcohol oxidation by **1** is a directed hydride abstraction, and even with an oxidant as weak as acetone, and under these mild conditions re-oxidation of intermediate ruthenium hydride **2** is rapid relative to k_2. We also find that substituting even one phenyl group on parent complex **1** significantly attenuates the oxidation reactivity. Using these insights we have discovered a rare example of C–H oxidation that occurs at a (formal) iron(0) center within the ligand–metal bifunctional scaffold. This offers significant potential advantages over ruthenium, such as cost, toxicity, and environmental impact. Further studies regarding directed hydride abstraction reactions are ongoing in our laboratory.

Experimental Section

General: General procedures and instrumentation are defined fully in the Supporting Information. Preparative details for all other materials and graphical ^{1}H NMR spectra are provided in the Supporting Information. [D_6]Benzene was vacuum-distilled from sodium/benzophenone ketyl for kinetics experiments. [D_6]Acetone was use as received from Alfa Aesar. Shvo's catalyst (**1**) was purchased from Strem and used as received. Pentacarbonyliron(0) [$Fe(CO)_5$] and nonacarbonyldiiron(0) [$Fe_2(CO)_9$] were purchased from Strem, manipulated under air-free conditions and protected from light. Benzoquinone was recrystallized from ethanol and used as a yellow crystal. Alcohols **6a**–**d** were purchased from common suppliers and distilled on a small scale immediately prior to use. Compound **9a** is commercially available, and compounds **9b**–**e** are known.[11] Spectroscopy and data: NMR spectra were measured with a Varian Mercury 400 NMR spectrometer. NMR spectroscopic data were processed and analyzed with Varian vnmr 6.1c or Acorn NMR NUTS. Spectra acquired for kinetics analysis were taken with a 5 s pulse sequence ($> 5 \times T1$). Charts and graphs were generated with Synergy Software KaleidaGraph 4. Error values were calculated and propagated by using traditional methods.

Kinetics: Sample procedure: A standard solution of Shvo's catalyst **1** (700 μL, 1.5 mM 1, in [D_6]acetone) was added to an oven-dried screw-cap NMR tube. No further precautions were taken to exclude air or water. The sample was placed into the NMR spectrometer pre-warmed to 323(1) K, and 10.2 μL (1.01 mmol, to make 120 mM, 2.5 mol-% Ru atom) of alcohol **6a** was added by syringe, and timing begun. The tube was reinserted into the NMR spectrometer. Integrations were recorded in comparison to a 1,2-dichloroethane (4.7 μL) internal standard. Kinetic constants (pseudo-first order k_{obs}) were determined by statistical agreement of k_{obs} values measured individually for aryl, methyl, benzyl (**6a**), and isopropyl C–H signals in multiple runs. Air sensitivity: For the case of ruthenium complexes, independence of rate from air and water exposure was verified by side-by-side runs conducted in [D_6]benzene with benzoquinone. One was prepared from solvent distilled from sodium/benzophenone ketyl and manipulated under air-free conditions, and the other was prepared with commercial materials on the bench top. Rate constants observed in these experiments were identical within error. This was not repeated in [D_6]acetone because anhydrous acetone is known to undergo dehydrative dimerization.[21] Kinetic isotope effects: Internal competition KIEs (k_H/k_D) were measured by comparison of [benzaldehyde] and [[D]benzaldehyde] as observed in ^{1}H NMR integrations for benzaldehyde and [D]benzyl alcohol. For catalyst **1**, 25 points throughout the first 40% of conversion were used. For complex **12**, 4 points through 20% conversion were used. Error was calculated as the standard deviation of these measurements. To insure comparability of integrations, spectra were acquired with a calibrated 90° pulse, 5 s ac-

Table 4. Kinetic dependence on [**1**] as shown in Figure 1 (left).

Entry	[**1**] [mM]	k_{obs} ($\times 10^5$ s^{-1})	ln [**1**]	ln(k_{obs})
1	1.50	7.55(26)	–6.50	–9.49(3)
2	2.90	11.1(1)	–5.84	–9.11(1)
3	4.50	11.6(1)	–5.40	–9.06(1)
4	6.50	14.1(1)	–5.04	–8.87(1)

Table 5. Kinetic dependence on [acetone] as shown in Figure 1 (right).

Entry	[acetone] [M]	k_{obs} ($\times 10^5$ s^{-1})
1	13.6 (100 vol.-%)	7.55(26)
2	10.2 (75 vol.-%)	6.74(58)
3	6.80 (50 vol.-%)	6.12(12)
4	3.40 (25 vol.-%)	5.82(13)

Table 6. Data for Hammett plot (Figure 2).

Entry	Alcohol: R	σ[7]	k_{obs} ($\times 10^5$ s^{-1})	ln(k_{obs})
1	**6b**: OMe	–0.268(77)	12.8(2)	0.228(15)
2	**6c**: Me	–0.170(46)	11.0(2)	0.164(17)
3	**6a**: H	0.000(34)	7.55(26)	0.000(20)
4	**6d**: F	+0.062(66)	6.53(11)	–0.063(32)

quisition time, and 45 s pulse delay. A control spectrum of [H_6]benzaldehyde showed < 5% error in ^{1}H integrations under these conditions (Tables 4, 5, and 6).

Preparative Details: Sample procedure of the oxidation of 1-phenylethanol: **1** (21.7 mg, 20.0 μmol), acetone (3 mL), and **6a** (121 μL, 1.00 mmol) were combined in a test tube with a stir bar. The resulting solution was subjected to reflux for 2 d, and the reaction mixture was cooled to room temperature, concentrated, and purified by flash column chromatography to afford **7a** (118 mg, 97%) as a colorless liquid.

Synthesis of 11: By cannulation, a 25 mL solution of **10**[22] (0.42 g, 2.00 mmol) in NEt_3 was added to a 25 mL solution of 4-iodotoluene (1.09 g, 5.01 mmol), [$PdCl_2(PPh_3)_2$] (0.03 g, 0.04 mmol), and [CuI] (0.02 g, 0.10 mmol) under nitrogen. The mixture was stirred at room temperature for 18 h at which time all volatiles were removed under reduced pressure. The resulting oil was dissolved in CH_2Cl_2 and washed once each with ca. 20 mL of $Na_2S_2O_3$ solution and brine, respectively. The organic layer was then dried with $MgSO_4$. Upon removal of all volatiles under reduced pressure, a golden-colored oil resulted. The oil was dissolved in 20 mL of hexanes and placed in a –15 °C freezer overnight. The product was isolated and recrystallized from hexanes resulting in 0.37 g (57% yield) of off-white crystals of **10a**; m.p. 68–71 °C. ^{1}H NMR ([D]-chloroform, 400 MHz): δ = 7.28 (d, $^3J_{H,H}$ = 7.5 Hz, 4 H, Ar-H), 7.09 (d, $^3J_{H,H}$ = 7.5 Hz, 4 H, Ar-H), 3.80 (s, 6H. OCH_3), 3.26 (s, 4 H, CH_2), 2.34 (s, 6 H, CH_3) ppm. ^{13}C NMR ([D]chloroform, 100 MHz): δ = 169.5 (2 C), 138.2 (2 C), 131.6 (4 C), 129.0 (4 C), 120.0 (2 C), 83.9 (2 C), 83.2 (2 C), 57.3, 53.1 (2 C), 23.9 (2 C), 21.5 (2 C) ppm. FTIR (NaCl): $\tilde{\nu}$ = 3291 (w), 3030 (w), 2954 (m), 2923 (w), 1743 (s), 1734 (s), 1511 (s), 1436 (m), 1327 (m), 1294 (m), 1263 (m), 1212 (br., s), 1107 (w), 1076 (m), 1058 (m), 1022 (w), 991 (w), 943 (w), 853 (w), 817 (s), 668 (w) cm^{-1}. $C_{25}H_{24}O_4$ (388.46): calcd. C 77.30, H 6.23; found C 76.73, H 6.11. The reaction was run air-free in a method similar to that described by Pearson et al.[18] Specifically, **10a** (0.11 g, 0.27 mmol) was dissolved in 600 mL of toluene (distilled from calcium hydride) in a 50 mL Strauss flask equipped with a stir bar. Next, [$Fe(CO)_5$] (0.22 mL, 1.63 mmol), previously degassed with N_2 was syringed into the flask. The flask was then flushed three times with CO gas and tightly sealed and placed into a 110 °C oil bath for 4 d. All volitales were then removed under reduced pressure, resulting in the crude product as a powdery solid. The solid was treated with warm hexanes and filtered, resulting in 80 mg (55% yield) of pure **11** as a mustard-yellow solid; decomposition 201–204 °C. ^{1}H NMR ([D]chloroform, 400 MHz): δ = 7.94 (d, $^3J_{H,H}$ = 7.9 Hz, 4 H, Ar-H), 7.23 (d, $^3J_{H,H}$ = 7.5 Hz, 4 H, Ar-H), 4.22 (d, $^2J_{H,H}$ = 16.6 Hz, 2 H, CH_2), 3.52 (d, $^2J_{H,H}$ = 16.6 Hz, 2 H, CH_2), 3.92 (s, 3 H, OCH_3), 3.89 (s, 3 H, OCH_3), 2.38 (apparent s, 6 H, CH_3) ppm. FTIR (NaCl): $\tilde{\nu}$ = 3437 (br., s), 2067 (s), 2029 (m), 1987 (s), 1739 (m), 1653 (m), 1645 (m), 1623 (s), 1309 (w), 1260 (w), 1206 (w), 1189 (w), 1166 (m), 1134 (w), 1050 (w), 872 (w), 822 (m), 752 (w), 732 (w), 711 (w), 615 (m), 588 (w), 568 (w) cm^{-1}. $C_{29}H_{24}FeO_8$ (556.34): calcd. C 62.61, H, 4.35; found C 62.76, H 4.35.

Supporting Information (see footnote on the first page of this article): Complete general procedures, details of kinetics analysis (including graphical spectra), preparative details and graphical spectra for new compounds, and line-listed X-ray crystallographic data for **11**.

Acknowledgments

This research was supported by the University of Southern California, the Loker Hydrocarbon Research Institute, and the ACS Petroleum Research Fund (grant 47987-G1). We thank Robert Bau and Tim Stewart for assistance with X-ray crystallography. T. J. W. thanks colleagues for insightful discussions: Kyung Jung, Surya Prakash, Mark Thompson, George Olah, Charles McKenna, Richard Brutchey, Tom Flood, and Nicos Petasis.

[1] Regarding hydride transfer, see: a) N. C. Deno, H. J. Peterson, G. S. Saines, *Chem. Rev.* **1960**, *60*, 7–14. Some examples include: b) Z. Li, D. S. Bohle, C.-J. Li, *Proc. Natl. Acad. Sci. USA* **2006**, *103*, 8928–8933; c) S. J. Pastine, K. M. McQuaid, D. Sames, *J. Am. Chem. Soc.* **2005**, *127*, 12180–12181; d) W. H. N. Nijhuis, W. Verboom, A. A. El-Fadl, S. Harkema, D. N. Reinhoudt, *J. Org. Chem.* **1989**, *54*, 199–209. via SET:; e) S. Fukuzumi, K. Ohkubo, T. Okamoto, *J. Am. Chem. Soc.* **2002**, *124*, 14147–14155; f) for a review, see: J.-E. Bäckvall, *J. Organomet. Chem.* **2002**, *652*, 105–111.

[2] Y. Blum, D. Czarkie, Y. Rahamim, Y. Shvo, *Organometallics* **1985**, *4*, 1459–1461.

[3] a) M. L. S. Almeida, M. Beller, G.-Z. Wang, J.-E. Bäckvall, *Chem. Eur. J.* **1996**, *2*, 1533–1536; b) J. B. Johnson, J.-E. Bäckvall, *J. Org. Chem.* **2003**, *68*, 7681–7684.

[4] a) C. P. Casey, S. E. Beetner, J. B. Johnson, *J. Am. Chem. Soc.* **2008**, *130*, 2285–2295; b) C. P. Casey, S. W. Singer, D. R. Powell, R. K. Hayashi, M. Kavana, *J. Am. Chem. Soc.* **2001**, *123*, 1090–1100.

[5] For a computational study of **1**-catalyzed hydrogenation of ketones, see: A. Comas-Vives, G. Ujaque, A. Lledós, *Organometallics* **2007**, *26*, 4135–4144.

[6] Further information on the synthetic applications of **1** and its related system [$(PPh_3)_2RuCl_2$]/K_2CO_3 has been reported: M. L. S. Almeida, M. Beller, G.-Z. Wang, J.-E. Bäckvall, *Chem. Eur. J.* **1996**, *2*, 1533–1536.

[7] L. P. Hammett, *J. Am. Chem. Soc.* **1937**, *59*, 96–103.

[8] K. Kaneda, K. Mori, T. Hara, T. Mizugaki, K. Ebitani, *Catal. Surv. Asia* **2004**, *8*, 231–239.

[9] K. Vijayasri, J. Rajaram, J. C. Kuriacose, *J. Mol. Catal.* **1987**, *39*, 203–217.

[10] H. B. Özgün, N. Değirmenbaşi, *J. Chem. Res. (S)* **1997**, 32–33.

[11] P. A. Wender, T. J. Paxton, T. J. Williams, *J. Am. Chem. Soc.* **2006**, *128*, 14814–14815.

[12] J. T. Groves, Y.-Z. Han, in *Cytochrome P450: Structure, Mechanism, and Biochemistry*, 2nd ed. (Ed.: P. R. Ortiz de Montellano), Plenum Press, New York, **1995**.

[13] a) M. Costas, M. P. Mehn, M. P. Jensen, L. Que Jr, *Chem. Rev.* **2004**, *104*, 939–986; b) M. M. Abu-Omar, A. Loaiza, N. Hontzeas, *Chem. Rev.* **2005**, *105*, 2227–2252. Regarding the first mechanistic evidence implicating the role of a non-heme Fe^V=O species in alkane hydroxylation, see: c) K. Chen, L. Que Jr, *J. Am. Chem. Soc.* **2001**, *123*, 6327 –6337.

[14] a) A. Company, L. Gómez, X. Fontrodona, X. Ribas, M. Costas, *Chem. Eur. J.* **2008**, *14*, 5727–5731; b) P. C. A. Bruijnincx, I. L. C. Buurmans, S. Gosiewska, M. A. H. Moelands, M. Lutz, A. L. Spek, G. van Koten, R. J. M. Klein Gebbink, *Chem. Eur. J.* **2008**, *14*, 1228–1237; c) M. S. Chen, M. C. White, *Science* **2007**, *318*, 783–787; d) G. J. P. Britovsek, J. England, S. K. Spitzmesser, A. J. P. White, D. J. Williams, *Dalton Trans.* **2005**, 945–955.

[15] S. Enthaler, G. Erre, M. K. Tse, K. Junge, M. Beller, *Tetrahedron Lett.* **2006**, *47*, 8095–8099.

[16] C. Bianchini, E. Farnetti, M. Graziani, M. Peruzzini, A. Polo, *Organometallics* **1993**, *12*, 3753–3761.

[17] Regarding a cyclopentadienone-ligated iron(II) catalyst for ketone hydrogenation, see: a) C. P. Casey, H. Guan, *J. Am. Chem. Soc.* **2007**, *129*, 5816–5817; b) H.-J. Knölker, E. Baum, H. Goesmann, R. Klauss, *Angew. Chem. Int. Ed.* **1999**, *38*, 2064.

[18] Prepared according to a known procedure: A. J. Pearson, R. J. Shively, R. A. Dubbert, *Organometallics* **1992**, *11*, 4096–4104.

[19] Prepared from Ph_4C_5O and $[Fe_2(CO)_9]$: G. N. Schrauzer, *J. Am. Chem. Soc.* **1959**, *81*, 5307–5310.
[20] CCDC-690601 contains the supplementary crystallographic data for this paper. These data can be obtained free of charge from The Cambridge Crystallographic Data Centre via www.ccdc.cam.ac.uk/data_request/cif.
[21] W. L. F. Armarego, C. L. L. Chai, *Purification of Laboratory Chemicals*, 5th ed., Elsevier, San Francisco, **2003**.
[22] R. S. Atkinson, M. J. Grimshire, *J. Chem. Soc. Perkin Trans. 1* **1986**, 1215–1224.

Received: October 6, 2008
Published Online: December 2, 2008

